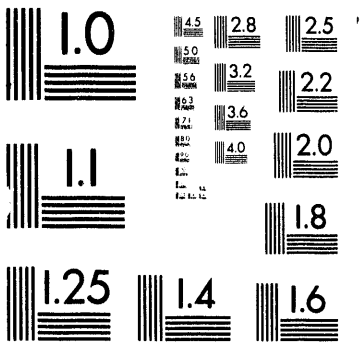
1.0
1.1
1.25
1.4
1.6
1.8
2.0
2.2
2.5
2.8
3.2
3.6
4.0
4.5
5.0
5.6
6.3
7.1
8.0

1 of 1

Conf-931108--20 SAND93-1529C

ELECTRIC-FIELD DEPENDENCE OF ELECTROREFLECTANCE AND PHOTOCURRENT SPECTRA AT VISIBLE WAVELENGTHS IN MOVPE-GROWN InAlGaP MULTIPLE STRAINED QUANTUM-WELL STRUCTURES

I. J. FRITZ, O. BLUM, R. P. SCHNEIDER, Jr., A. J. HOWARD AND D. M. FOLLSTAEDT,
Sandia National Laboratories, Albuquerque, NM 87185

ABSTRACT

We present electric-field dependent electroreflectance and photocurrent spectra of visible-bandgap $In_x(Al_yGa_{1-y})_{1-x}P/In_{x'}(Al_{y'}Ga_{1-y'})_{1-x'}P$ multiple-quantum-well (MQW) structures. These structures, grown by metal-organic vapor phase epitaxy on 6°-misoriented (100) GaAs substrates, have undoped MQWs sandwiched between doped $In_{0.5}Al_{0.5}P$ layers, forming p-i-n diodes. Quantum-well compositions in the range $0.46 \le x \le 0.52$ and $0 \le y \le 0.4$, corresponding to bandgaps in the red to yellow-green range, were used. The Stark shifts in these various samples were measured and found to depend on the details of the Mg p-type doping profile, confirming important diffusion effects, in agreement with secondary ion mass spectrometry and capacitance-voltage data. Our results show that these new materials are promising for visible-wavelength optical modulator applications.

Materials from the InAlGaP system grown on GaAs substrates have potential optoelectronic applications at visible wavelengths in the green to red range. Recent successful development of vertical-cavity surface-emitting lasers[1] and resonant-cavity light-emitting diodes[2] suggest that vertical-cavity electro-optic modulators[3] should also be feasible with these materials. Optical modulators generally operate from the large near-bandgap changes of absorption and refractive index induced by electric fields in quantum-well structures (i.e., the quantum-confined Stark effect,[4] or QCSE), but field effects in InAlGaP heterostructures have not been studied yet. It is not obvious whether material optimized for emitters will be suitable for modulator applications. While high-temperature and off-axis growth have eliminated sublattice ordering,[5] these materials still have nano-scale compositional variations, as seen in transmission electron micrographs.[6] Furthermore, issues of dopant incorporation and diffusion in these materials have only recently begun to be addressed and are crucial for modulator development.

The conditions of our low-pressure MOVPE growth have been described previously.[5] To minimize sublattice ordering, we grew at 775 °C on GaAs substrates misoriented 6° from (001) towards the nearest {111}A. A schematic of our samples is given in Fig. 1. The 0.5-μm thick active regions consist of 25.5 periods of nominally undoped $In_x(Al_yGa_{1-y})_{1-x}P/In_{x'}(Al_{y'}Ga_{1-y'})_{1-x'}P$ multiple quantum wells (MQWs). Surrounding the active regions are n- and p-type cladding layers of InAlP (lattice matched to the GaAs substrate). The lower cladding layers are 0.6 μm thick, doped to 2×10^{18} cm^{-3} with Si, while the upper ones are 0.2 μm thick, doped to 8×10^{17} cm^{-3} with Mg.

In Table I we give more details of the four individual samples (A-D) studied here. Sample A has tensilely strained (0.3%) $In_{0.46}Ga_{0.54}P$ quantum wells and compressively strained (0.3%) $In_{0.52}(Al_{0.7}Ga_{0.3})_{0.48}P$ barriers. Sample B has compressively strained $In_{0.52}(Al_{0.4}Ga_{0.6})_{0.48}P$ quaternary quantum wells and tensilely strained

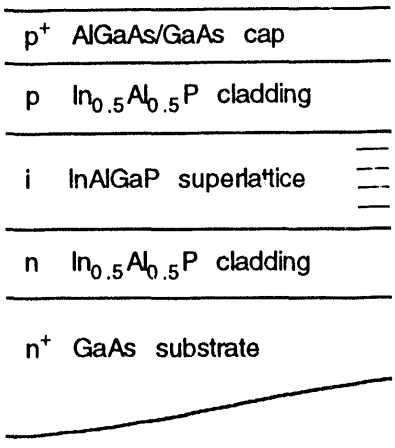

Fig. 1. Schematic of the quantum-well structures studied.

$In_{0.46}(Al_{0.7}Ga_{0.3})_{0.54}P$ barriers. Samples C and D have unstrained layers of $In_{0.49}Ga_{0.51}P$ and $In_{0.49}(Al_{0.5}Ga_{0.5})_{0.51}P$ in their MQWs. These samples are identical except that sample D has a nominally undoped setback layer, 100 nm thick, adjacent to the MQW region in the upper cladding layer. This setback layer was included to reduce possible Mg diffusion into the MQW region. We list the bandgap wavelengths of our four samples, as determined from room-temperature photoluminescence, in the last column of Table I. The bandgaps span the range from red (640 nm) to yellow-green (583 nm).

Sample A was studied by <011> cross-section transmission electron microscopy (TEM). The diffraction pattern showed no evidence of sublattice ordering, consistent with the high growth temperature and misoriented substrate. Diffraction from the MQW superlattice was observed and yielded a periodicity in agreement with the target values of Table I. The TEM images show an irregular wavy contrast on a scale of ~10 nm - 100 nm, as seen in Fig. 2. The exact origin of this structure is not known, but is likely due to compositional variations, e.g. a spinodal-like decomposition.[6]

Mesa-isolated devices were fabricated with standard photolithographic techniques, with a H_3PO_4:H_2O_2:H_2O (1:4:45) etch for the GaAs/AlGaAs cap layer, followed by an H_3PO_4:HCl:H_2O (10:5:3) etch for the phosphide materials.[7] Rings of Ti/Au contacted the p-type GaAs cap layers and GeNiAu contacted the substrate side of the wafers. Electroreflectance (ER) spectra were taken at room temperature at various dc bias levels with a 0.4-V peak-to-peak square wave voltage modulation superimposed. Spectra were taken at 0.5 V intervals between 1 V and -1 V applied dc bias, and at 1 V intervals between -1 V and -7 V (samples A and B) or -8 V (samples C and D). Where 1 V intervals were employed, linearly interpolated spectra were generated at 0.5 V intervals to smoothen the appearance of surface and contour plots of the data. Room-temperature photocurrent (PC) spectra as a function of bias were obtained using chopped light to reduce noise caused by voltage fluctuations.

A two-band envelope-function calculation was used to predict the energies of the various

Table I. Structural and compositional parameters for the present samples, along with the band-gap wavelengths determined from room-temperature photoluminescence.

	Quantum well			Barrier			p-doping	
Sample	x	y	d_w (nm)	x'	y'	d_b (nm)	setback (nm)	Bandgap (nm)
A	0.46	0	10.6	0.52	0.7	9.4	0	630
B	0.52	0.4	9.4	0.46	0.7	10.6	0	583
C	0.49	0	10.0	0.49	0.5	10.0	0	640
D	0.49	0	10.0	0.49	0.5	10.0	100	640

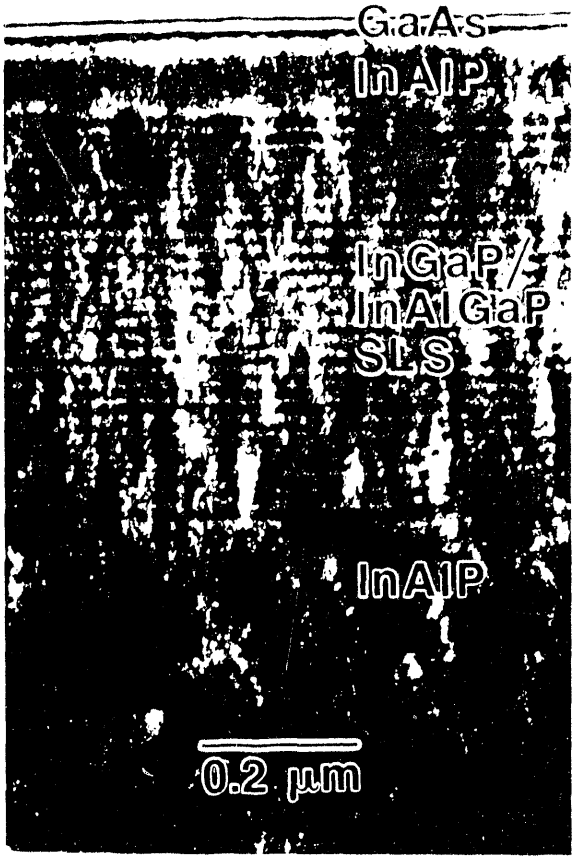

Fig. 2. TEM micrograph of sample A.

quantum well transitions.[8] Parameters in this calculation are similar to those used recently by other workers.[9] To calculate the electric-field induced energy level shifts, we use a tunneling resonance calculation again in the two-band envelope-function approximation.

Representative data from sample A are shown in Fig. 3. Curve (a) is the zero-bias PC spectrum, curve (b) the zero-bias ER spectrum, and curve (c) the −3 V ER spectrum. We have indicated the calculated positions of several quantum well transitions, using the notation ijk, where i = electron quantum level index, j = hole index, and k = H (heavy hole) or L (light hole). We see that there are distinct spectral features in both the ER and PC spectra near the predicted i = j heavy-hole transitions, but that the light-hole transitions are not separately resolved. For the structures studied here, the 1HH to 1LH separation is predicted to be small (< 3 nm). Additional spectral features in curve (b) appear due to a superposition of several rather broad and overlapping transitions.

In ER spectra, transitions with both i ≠ 1 and j ≠ 1 tend to be weak, because the Stark shifts for these transitions are much smaller than for transitions involving ground-state levels. Thus for large electric fields, where the i ≠ j transitions become allowed, we expect the 2HH and 12H transitions to dominate the above-gap spectra.[10] The predicted positions of these transitions are marked on the −3 V spectrum and are in reasonable agreement with the positions of observed lines.

In Fig. 4 we show the bias dependence of the photocurrent spectrum of sample A. With increasing electric field, the spectra broaden and shift to longer wavelength, as expected from the QCSE. Note that near 660 nm there is a significant change in absorption with bias that could be used in modulator device applications. The quenching of the band-edge exciton with field is quite rapid in the present samples due to the large effective masses in these materials (compared, e.g., to GaAs quantum wells) and also to field non-uniformities stemming from Mg dopant diffusion.

Because of its derivative nature, ER spectroscopy gives a clearer view of the electric-field effects than does PC spectroscopy. We demonstrate this advantage in Figs. 5 and 6, which show contours of the ER signal vs. wavelength and bias for the four samples of Table I. For clarity we show only the positive ER signal, which is sufficient for illustrating the Stark shifts.

Data from sample A are shown in Fig. 5a. The band-edge transition (near 650 nm) shifts strongly with field for reverse bias beyond −1 V. However, for biases in the −1 V to +2 V range, the spectra are anomalous, with the band-edge transition shifted to wavelengths similar to those observed near −2 V bias. We believe this shift may be caused by formation of a built-in field domain in the MQW region, an occurrence that is well known in MQWs and superlattices with significant carrier density.[11] Consistent with this interpretation, the capacitance–voltage (C–V) profile of

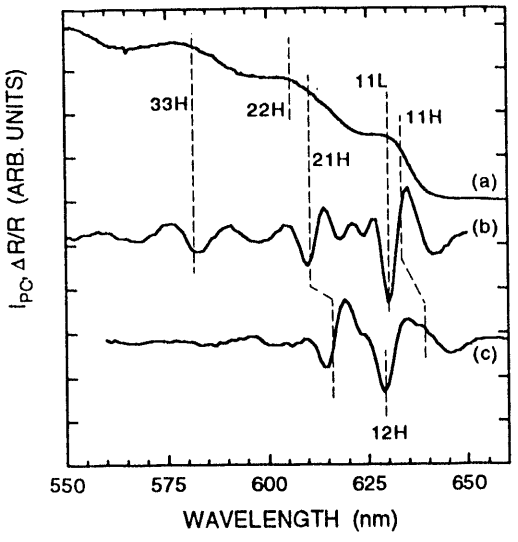

Fig. 3. Photocurrent (a) and electroreflectance spectra (b) and (c) of sample A. Curves (a) and (b) taken at 0 V bias, curve (c) at -3 V.

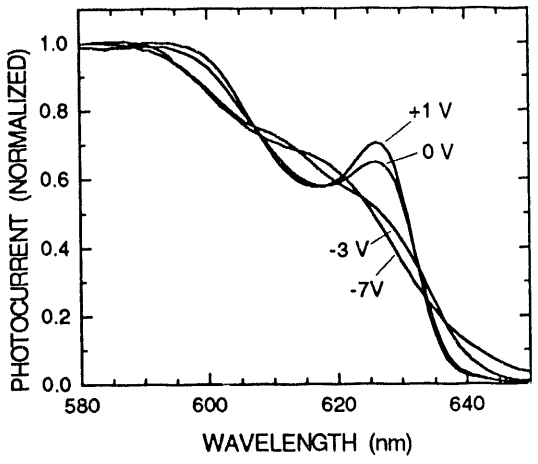

Fig. 4. Photocurrent spectra of sample A at various bias voltages.

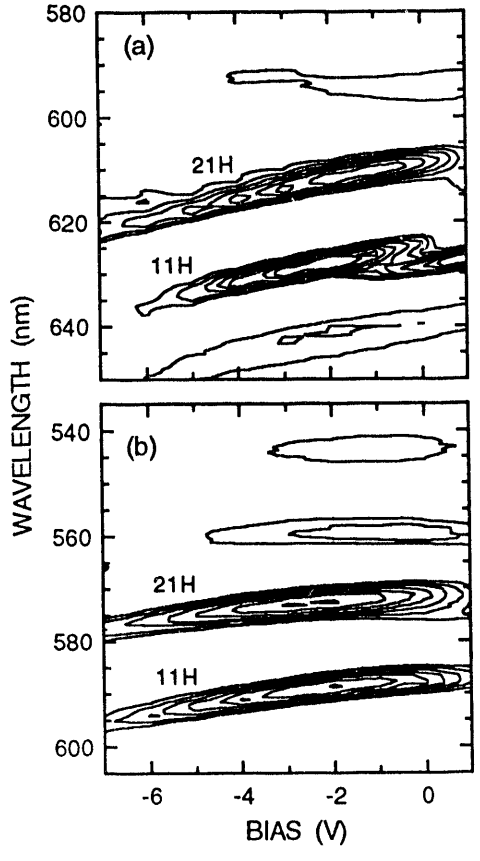

Fig. 5. Countours of electroreflectance vs. wavelength and bias for (a) sample A and (b) sample B.

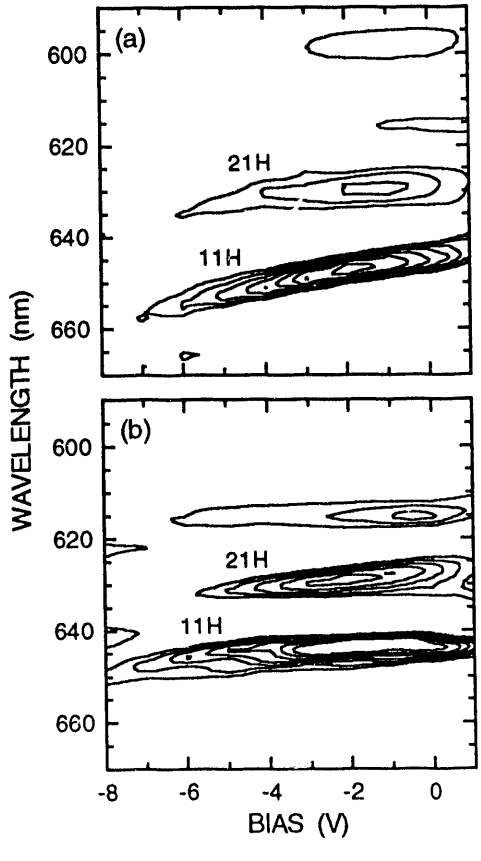

Fig. 6. Electroreflectance contours of (a) sample C and (b) sample D.

this sample shows a slow depletion with bias voltage and a relatively high background doping level (~$3x10^{16}cm^{-3}$). The presence of possible space charge regions in the sample makes estimates of the electric field at various bias voltages somewhat uncertain. Nevertheless, the overall trend in the position of the bandgap with bias agrees with our calculations and demonstrates that a strong QCSE can be achieved in InAlGaP quantum-wells. Figure 5b gives the results on sample B, which has quaternary quantum wells and demonstrates that a significant Stark shift can be observed (587 nm to 596 nm with 7 V of reverse bias) at yellow-green wavelengths despite rather shallow quantum wells.

The ER contours for sample C are shown in Fig. 6a. The Stark shift of ~15 nm (44 meV) is clearly visible. Figure 6b illustrates the results from sample D. This sample is identical to sample C, except for the doping setback, but the bias dependence of its ER spectrum is significantly different, with a total Stark shift of only ~5 nm. The striking difference between samples C and D reflect the importance of background doping and dopant diffusion in our p-i-n diode structures.[12] The Mg doping profiles obtained from secondary ion mass spectrometry (SIMS) in sample C show a Mg doping tail extending ~150 nm into the MQW region. Although this doping tail causes some electric field inhomogeneity in the MQW, the C-V profile shows that ~400 nm of the MQW (i.e., 80% of the total thickness) is depleted at 0 V bias, so that large fields are present at reverse biases, explaining the achievement of large Stark shifts.

In contrast, the SIMS results on sample D show no Mg tail in either the setback layer or the MQW, but instead a higher, nearly constant Mg background (~$2x10^{16}cm^{-3}$) in these regions. The C-V profile shows a very slow depletion with bias, requiring -3 V for significant depletion. In addition, the capacitance has an anomalous frequency dependence, suggesting possible slow charge transport in the structure. These C-V anomalies may be related to the different background doping levels in the cladding and superlattice regions, which remain to be characterized. For example, a large n-type background in the cladding layer could produce a potential barrier opposing the applied bias field, thereby explaining the lack of a uniform field and the resultant small Stark shift.

In summary, we have studied electric-field effects in a variety of InAlGaP quantum-well structures including structures with quaternary quantum wells and structures with strain in both quantum-well and barrier layers. Our results show that well-defined Stark shifts can be observed in samples with bandgaps in the red to yellow-green wavelength range. Background doping and dopant diffusion effects have been observed with SIMS and C-V profiling and generally correlate with degradation of the Stark effect. Our results demonstrate that InAlGaP materials are promising candidates for optical modulator devices at visible wavelengths.

ACKNOWLEDGMENTS

We are grateful to L. Griego, R. J. Winkleman, J. J. Figiel, M. P. Moran and J. M. Sergeant for expert technical assistance. This work was supported by the U. S. Department of Energy under Contract DE-AC04-94AL85000.

REFERENCES

1. R. P. Schneider, Jr., R. P. Bryan, J. A. Lott and G. R. Olbright, Appl. Phys. Lett. **60**, 1830 (1992); J. A. Lott and R. P. Schneider, Jr., Electron Lett. **29**, 830 (1993).

2. J. A. Lott, R. P. Schneider, Jr., J. C. Zolper and K. J. Malloy, IEEE Photon. Technol. Lett. **5**, 631 (1993).

3. M. Whitehead and G. Parry, Electron. Lett. **25**, 568 (1989).

4. D. A. B. Miller, D. S. Chemla, T. C. Damen, A. C. Gossard, W. Wiegmann, T. H. Wood and C. A. Burrus, Phys. Rev. **B32**, 1043 (1985).

5. R. P. Schneider, Jr., E. D. Jones, J. A. Lott and R. P. Bryan, J. Appl. Phys. **72**, 5397 (1992).

6. D. M. Follstaedt, R. P. Schneider, Jr. and E. D. Jones, Procedings of the Fall 1993 Materials Research Society, to be published.

7. J. R. Lothian, J. M. Kuo, W. S. Hobson, E. Lane, F. Ren and S. J. Pearton, J. Vac. Sci. Technol. B **10**, 1061 (1992); J. R. Lothian, J. M. Kuo, F. Ren and S. J. Pearton, J. Electron. Mater. **21**, 441 (1992).

8. I. J. Fritz, J. F. Klem, T. M. Brennan, J. R. Wendt and T. E. Zipperian, Supperlatt. and Microstr. **10**, 99 (1991).

9. R. P. Schneider, Jr., R. P. Bryan, E. D. Jones and J. A. Lott, Appl. Phys. Lett. **63**, 1240 (1993).

10. I. J. Fritz, T. M. Brennan, J. R. Wendt and D. S. Ginley, Appl. Phys. Lett. **57**, 1245 (1990).

11. H. T. Grahn, H. Schneider and K. von Klitzing, Phys. Rev. B **41**, 2890 (1990).

12. I. J. Fritz, O. Blum, R. P. Schneider, Jr., A. J. Howard and D. M. Follstaedt, submitted to Appl. Phys. Lett.

DISCLAIMER

DATE FILMED

1/31/94

END